

Fragileness of Exact I-ball/Oscillon

Masahiro Ibe,^{1,2,*} Masahiro Kawasaki,^{1,2,†}

Wakutaka Nakano,^{1,2,‡} and Eisuke Sonomoto^{1,2,§}

¹*ICRR, The University of Tokyo, Kashiwa, Chiba 277-8582, Japan*

²*Kavli IPMU (WPI), UTIAS, The University of Tokyo, Kashiwa, Chiba 277-8583, Japan*

(Dated: August 2019)

Abstract

I-ball/oscillon is a soliton-like oscillating configuration of a real scalar field which lasts for a long time. I-ball/oscillon is a minimum energy state for a given adiabatic invariant, and its approximate conservation guarantees the longevity. In this paper, we examine the stability of a special type of I-ball/oscillon, the “exact” I-ball/oscillon, whose adiabatic invariant is exactly conserved. We show that the exact I-ball/oscillon is stable in classical field theory, but not stable against small perturbations depending on the value of its adiabatic invariant. Accordingly, the exact I-ball/oscillon breaks up in the presence of the fluctuations with corresponding instability modes. We also confirm the fragileness of the exact I-ball/oscillon by the classical lattice simulation.

arXiv:1908.11103v1 [hep-ph] 29 Aug 2019

* e-mail: ibe@icrr.u-tokyo.ac.jp

† e-mail: kawasaki@icrr.u-tokyo.ac.jp

‡ e-mail: m156077@icrr.u-tokyo.ac.jp

§ e-mail: sonomoto@icrr.u-tokyo.ac.jp

I. INTRODUCTION

I-ball/oscillon is a non-topological soliton-like solution in real scalar field theory [1–3] whose formation process is nonlinear. This lump of a real scalar field is a minimum energy state and understood as the coherent oscillation around the (local) minimum of the potential. A lot of studies on the I-ball/oscillon [4–27] indicate that the lifetime of I-ball/oscillon is extremely long. The longevity of the I-ball/oscillon could leave an imprint on cosmology/astrophysics which can be tested by some experiments. (See e.g. [28–30] for gravitational waves from the I-ball/oscillon. See also [31].)

The longevity of I-ball/oscillon is guaranteed by the approximate conservation of adiabatic invariant I [13, 32]. The adiabatic invariance is the analog to the invariance of the phase space volume for a periodic motion in classical mechanics. It is also known that the adiabatic invariant corresponds to the particle number [33] in the non-relativistic limit, and hence, the approximate conservation of I is regarded as the particle number conservation in this limit.

In this paper, we study the stability of a special type of the I-ball/oscillon, the “exact” I-ball/oscillon, which appears in a real scalar theory with a particular type of potential [13]. In this particular case, the adiabatic invariant of I-ball/oscillon is exactly conserved. We show that the exact I-ball/oscillon is stable in classical field theory. We also find that the exact I-ball/oscillon is not stable against small perturbations depending on the value of the adiabatic invariant. Accordingly, the exact I-ball/oscillon breaks up in the presence of the fluctuations corresponding to the instability modes. We also confirm the fragileness of the exact I-ball/oscillon by the classical lattice simulation.

Organization of this paper is as follows. In section II, we introduce the exact I-ball/oscillon, which conserves the adiabatic invariant exactly. In section III, we show that the exact I-ball/oscillon is stable, but the perturbation around it has resonance bands and it breaks the exact I-ball/oscillon depending on its parameters. In section IV, we show the setup and the result of our lattice simulation to confirm fragileness of the exact I-ball/oscillon. Finally, in section V, we conclude the results.

II. EXACT I-BALL/OSCILLON

A. Exact conservation of adiabatic invariant

I-ball/oscillon is a localized oscillating scalar field configuration which minimizes the energy for a given value of the adiabatic invariant I . The adiabatic invariant of a real scalar field ϕ is defined by

$$I = \frac{1}{\omega} \int d^3x \overline{\phi^2}, \quad (1)$$

where ω is the angular frequency of the oscillating field and the overbar denotes the average over one period of the oscillation.

The adiabatic invariant Eq. (1) is approximately conserved when the scalar field oscillates in the potential dominated by the quadratic term ($\sim \phi^2$). In other words, the I-ball/oscillon is not an exact periodic motion in time, and hence, the time average over one period of the oscillation in Eq. (1) is not exact. Due to this approximate conservation of I , I-ball/oscillon is generally quasi-stable and eventually decays by emitting scalar waves [25].

However, the adiabatic invariant is exactly conserved when the solution of the equation of motion is completely separable into the time and the spatial dependent parts [13].

Let us assume an I-ball/oscillon solution with the separated form as

$$\phi(t, \vec{x}) = f(t)\psi(\mathbf{x}). \quad (2)$$

where $\psi(\mathbf{x})$ is the theoretical oscillon profile and $f(t)$ is a time periodic function normalized as $\max\{f(t)\} = 1$. The fact that the time and spatial dependencies are determined separately is crucial when we consider the I-ball/oscillon stability. In this case, the adiabatic invariant I is evaluated as

$$I = \frac{\overline{f^2}}{\omega} \int d^3x \psi(\mathbf{x})^2, \quad (3)$$

where overbar denotes the time average over the one period of oscillation. Because $f(t)$ is exactly periodic, the adiabatic invariant I is constant in time, and hence, is conserved exactly.

Such a separated solution like Eq. (2) is possible only when the scalar potential of ϕ takes the form of

$$V = \frac{1}{2}m^2\phi^2 + \Delta V = \frac{1}{2}m^2\phi^2 + \frac{1}{2}\kappa m^2\phi^2 \log \frac{\phi^2}{M^2}. \quad (4)$$

where $\kappa < 0$ is a dimensionless constant and m and M are mass parameters ¹ [13].

For a later purpose, we redefine the parameters by

$$\tilde{m}^2 = m^2 + \kappa m^2 \log \frac{\tilde{m}^2}{M^2} , \quad (5)$$

$$\tilde{\kappa} \tilde{m}^2 = \kappa m^2 , \quad (6)$$

with which

$$V = \frac{1}{2} \tilde{m}^2 \phi^2 + \frac{1}{2} \tilde{\kappa} \tilde{m}^2 \phi^2 \log \frac{\phi^2}{\tilde{m}^2} . \quad (7)$$

In what follows, we use the latter expression with $\tilde{m}^2 \rightarrow m^2$ and $\tilde{\kappa} \rightarrow \kappa$. Eventually, the potential depends only on two parameters, m and κ .

Substituting the solution Eq. (2) into the equation of motion

$$\ddot{\phi} - \nabla \phi + m^2 \phi + \Delta V' = 0 , \quad (8)$$

we obtain

$$\left[\ddot{f} + m^2 f + \kappa m^2 (1 + \log f^2) f \right] \psi - \left[\nabla \psi - \kappa m^2 \psi \log \frac{\psi^2}{m^2} \right] f = 0 . \quad (9)$$

This leads to the following two equations:

$$\ddot{f} + m^2 f + \kappa m^2 (1 + \log f^2) f = \zeta m^2 f , \quad (10)$$

$$\nabla^2 \psi - \left(\kappa m^2 \log \frac{\psi^2}{m^2} \right) \psi = \zeta m^2 \psi , \quad (11)$$

where ζ is a constant. As we will see in the next section, ζ determines the adiabatic invariant of the I-ball/oscillon for given potential parameters.

Therefore, because the solutions of equations of motions under the potential Eq. (4) are independently determined by Eqs. (10) and (11) the adiabatic invariant is exactly conserved ² as shown in Ref. [13].

B. The exact I-ball/oscillon solution

As the I-ball/oscillon corresponds to the minimum energy states for a given value of I , the I-ball/oscillon profile ψ is expected to be spherical, $\psi(\vec{x}) = \psi(r)$. Then, Eq. (11) has an

¹ The parameter M corresponds to the renormalization scale.

² From Eq. (10), we can evaluate $\overline{\dot{f}^2}$ as

$$\overline{\dot{f}^2} = m^2 (1 + \kappa - \zeta) \overline{f^2} + \kappa m^2 \overline{f^2 \log f^2} . \quad (12)$$

exact solution,

$$\psi(r) = \psi_c \exp(-r^2/R^2) , \quad (13)$$

where

$$R = \sqrt{\frac{2}{|\kappa|} \frac{1}{m}} , \quad (14)$$

$$\psi_c^2 = m^2 \exp\left(3 - \frac{\zeta}{\kappa}\right) . \quad (15)$$

ψ_c and R is the central value and the radius of the I-ball/oscillon. It should be noted that the spatial size of R does not depend on ζ , and hence, does not depend on I for given potential parameters.

The period of the oscillation can be obtained as follow. By multiplying \dot{f} to Eq. (10) and integrating over time t , we obtain

$$\frac{1}{2}\dot{f}^2 + \frac{1}{2}m^2(1 - \zeta)f^2 + \frac{1}{2}\kappa m^2 f^2 \log f^2 = C_f , \quad (16)$$

with C_f being a constant. Because the potential of f is a even function of f , f oscillates in $f = [-1, 1]$, and hence, C_f is required to be $C_f > 0$ to allow $\dot{f}^2 > 0$ at $f = 0$. As we defined $f = \pm 1$ at the turning points of the motion, C_f is represented by

$$C_f = \frac{1}{2}m^2(1 - \zeta) , \quad (17)$$

with which $\dot{f} = 0$ at the turning points. As a result, we find a period of the oscillation to be

$$T \equiv \frac{2\pi}{\omega} = 2 \int_{-1}^1 \frac{df}{\sqrt{m^2(1 - \zeta)(1 - f^2) - \kappa m^2 f^2 \log f^2}} , \quad (18)$$

which is determined by ζ for given potential parameters. We plot the frequencies for the potential parameter $\kappa = -0.3$ and $\kappa = -0.1$ in Fig. 1. The upper bound for the range of ζ is determined from Eq. (18) with $T = \text{finite}$,

$$\zeta_{\max} = 1 + \kappa \leq 1 . \quad (19)$$

Besides, the region of $\omega \geq m$ is not physically attractive³, and hence, we consider only closed range of ζ .

³ More precise lower bound on ζ is determined by $dE/dI < m$.

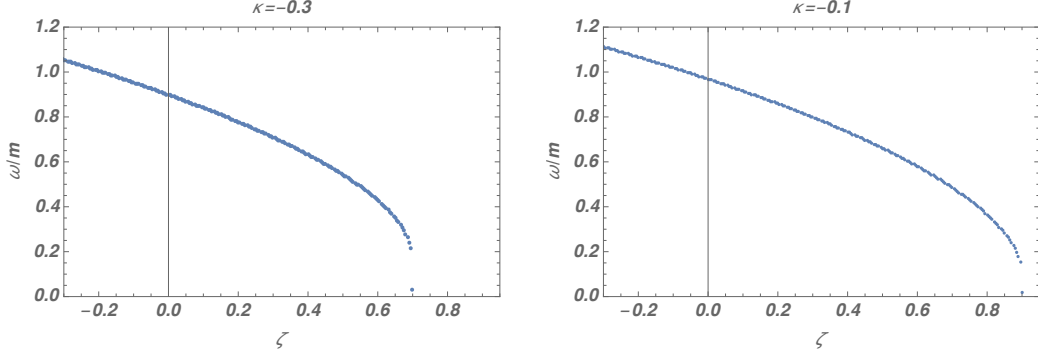


FIG. 1. (Left) The relation of ζ and ω for $\kappa = -0.3$. (Right) Same plot for $\kappa = -0.1$.

Similarly, the energy of the I-ball/oscillon is given by

$$E = \left(\overline{f^2} - \frac{1}{2} \kappa m^2 \overline{f^2} \right) \int d^3x \psi(r)^2, \quad (20)$$

$$= \left(1 - \frac{1}{2} \kappa m^2 \frac{\overline{f^2}}{\dot{f}^2} \right) \omega I, \quad (21)$$

where

$$I = \frac{\overline{f^2}}{\omega} \int d^3x \psi(r)^2 = \frac{\overline{f^2}}{m\omega} \left(\frac{\pi}{|\kappa|} \right)^{3/2} \frac{\psi_c^2}{m^2}. \quad (22)$$

Here, we used Eqs. (10), (3), and (12). Notice that $\overline{f^2}$, ω and ψ_c depend on ζ through Eqs. (12), (15) and (18). Thus, the adiabatic invariant is determined only by ζ for given model parameters κ and m .

III. STABILITY AND INSTABILITY OF THE EXACT I-BALL/OSCILLON

A. Stability

As shown in [25], the non-exact I-ball/oscillon decays by emitting relativistic radiation of the scalar field. Here, let us discuss whether the exact I-ball/oscillon obeys this decay process.

To see whether a relativistic radiation is emitted from the exact I-ball/oscillon, we consider a small perturbation around the I-ball/oscillon, $\phi(x) = \phi_I(x) + \xi(x)$. Here, $\phi_I(x)$ is the I-ball/oscillon solution obtained in the previous section. Then, the equation of motion of the perturbation $\xi(x)$ is given by

$$(\square + V'')|_{\phi=\phi_I} \xi(x) = \mathcal{O}(\xi(x)^2), \quad (23)$$

where

$$V'' = m^2 \left(1 + 3\kappa + \kappa \log \frac{\phi^2}{m^2} \right) . \quad (24)$$

Eq. (23) shows that the perturbation does not have source terms, and the I-ball/oscillon solution is stable if $\xi = 0$ initially. Thus, unlike the case of the non-exact I-ball/oscillon, the exact I-ball/oscillon does not decay by emitting relativistic radiations.

The absence of the source term of ξ stems from the fact that the equation for the I-ball/oscillon profile is the same as the equation of motion Eqs. (10) and (11) without averaging over one period of the oscillation. This contrasts with generic I-ball/oscillon solutions. In general cases, the I-ball/oscillon solutions satisfy the equation of motion only after averaging over a period, and hence, the perturbation has source terms coming from the potential which disappear if averaged. This leads to the decay of the I-ball/oscillon as shown in Ref. [25]. These observations are consistent with the exactness of the conservation of the adiabatic invariant.

B. Fragileness

In this subsection, we discuss the instability of the exact I-ball/oscillon against small perturbations and derive the growth index (the Floquet exponent) of the instability.

As $\kappa < 0$, the perturbation around the vacuum, i.e. $\phi = 0$, has an infinite mass, i.e. $m_\xi^2 = \infty > 0$.⁴ Thus, the perturbation around the vacuum is never excited. Around the I-ball/oscillon solution,

$$\phi_I(x) = f(t)\psi(r) , \quad \psi(r) = \psi_c e^{-r^2/R^2} , \quad (25)$$

on the other hand, the perturbation has a finite non-derivative kernel,

$$\ddot{\xi}(x) - \nabla^2 \xi(x) + \left(2|\kappa|m^2 \frac{r^2}{R^2} + (1 + 3\kappa)m^2 + \kappa m^2 \log \frac{\psi_c^2}{m^2} + F(t) \right) \xi(x) = 0 , \quad (26)$$

where $F(t) = \kappa m^2 \log f(t)^2$. and we neglected $\mathcal{O}(\xi^2)$ term in Eq. (23). Thus, there could be instability modes around the I-ball/oscillon solution.

⁴ The mass at the origin of this potential is divergent because

$$V''(\phi) = m^2 \left[(1 + 3\kappa) + \kappa \log \left(\frac{\phi}{m} \right)^2 \right] \rightarrow \infty. \quad (\phi \rightarrow \pm 0)$$

To analyze Eq. (26), let us remember that the eigenequation,

$$(-\nabla^2 + \omega_\xi^2 r^2) \lambda_{\mathbf{n}}(\mathbf{x}) = 2E_{\mathbf{n}} \lambda_{\mathbf{n}}(\mathbf{x}) , \quad (27)$$

has the eigenfunctions and eigenvalues,

$$\lambda_{\mathbf{n}}(\mathbf{x}) = \prod_{i=1}^3 \left(\frac{1}{n_i! 2^{n_i}} \sqrt{\frac{\omega_\xi}{\pi}} \right)^{1/2} H_{n_i}(\sqrt{\omega_\xi} x_i) e^{-\omega_\xi x_i^2/2} , \quad (28)$$

$$2E_{\mathbf{n}} = 2\omega_\xi(n_1 + n_2 + n_3 + 3/2) . \quad (29)$$

where H_n denotes the Hermite polynomial of order n , and the eigenfunctions satisfy $\lambda_{\mathbf{n}}(|\mathbf{x}| \rightarrow \infty) = 0$.

By expanding $\xi(x)$ by,

$$\xi(t, \mathbf{x}) = \sum_{\mathbf{n}} q_{\mathbf{n}}(t) \lambda_{\mathbf{n}}(\mathbf{x}) , \quad (30)$$

we find that each $q_{\mathbf{n}}(t)$ satisfies

$$[\partial_t^2 + 2\omega_\xi(n_1 + n_2 + n_3) + \Lambda + F(t)] q_{\mathbf{n}}(t) = 0 . \quad (31)$$

Here, we defined

$$\omega_\xi^2 = 2|\kappa| \frac{m^2}{R^2} = \kappa^2 m^4 , \quad (32)$$

$$\Lambda = (1 + 3\kappa)m^2 + \kappa m^2 \log \frac{\psi_c^2}{m^2} + 3\omega_\xi , \quad (33)$$

$$= (1 + 3\kappa - \zeta)m^2 , \quad (34)$$

where we used Eq. (15). The exponential factor in Eq. (28) is identical to that of the I-ball/oscillon, i.e.

$$e^{-\omega_\xi(x_1^2+x_2^2+x_3^2)/2} = e^{-r^2/R^2} . \quad (35)$$

If Eq. (31) has growing modes with non-trivial Floquet exponents, the I-ball/oscillon solution can be unstable.

It should be noted that the perturbation of the zero mode, $\mathbf{n} = 0$, is redundant. As the radius of the I-ball/oscillon does not depend on ζ but is determined by κ and m , the addition of the zero mode perturbation just enhances the value of I , which leads to an I-ball/oscillon with a slightly larger I .

Because we confine ourselves to the spherical configuration in our numerical simulation, we consider the spherical perturbations to analyze the result of our simulation.

Let us rewrite Eq. (27) in the spherical coordinate,

$$\left(-\frac{d^2}{dr^2} - \frac{2}{r} \frac{d}{dr} + \frac{\ell(\ell+1)}{r^2} + \omega_\xi r^2 \right) R_{n_r, \ell}(r) = 2E_{n_r, \ell} R_{n_r, \ell}(r) , \quad (36)$$

where the eigenfunction is given by $R_{n_r, \ell}(r) Y_m^\ell(\Omega)$ with $Y_m^\ell(\Omega)$ being the spherical harmonics. By introducing $\tilde{r} = \sqrt{\omega_\xi} r$, the eigenfunction of the radial direction and the corresponding energy are given by,

$$R_{n_r, \ell}(\tilde{r}) = \frac{2^{1/2} \omega_\xi^{3/2} \Gamma(n_r + \ell + 3/2)^{1/2}}{\Gamma(n_r + 1)^{1/2} \Gamma(\ell + 3/2)} \tilde{r}^\ell e^{-\tilde{r}^2/2} {}_1F_1(-n_r; 3/2 + \ell; \tilde{r}^2) , \quad (37)$$

$$2E_{n_r, \ell} = 2(2n_r + \ell + 3/2) , \quad (38)$$

for $(n_r = 0, 1, 2 \dots)$ and $(\ell = 0, 1, 2 \dots)$. Here, ${}_1F_1(a; b; z)$ denotes the confluent hypergeometric function, and the wave function is normalized so that

$$\int_0^\infty dr r^2 R_{n_r, \ell}(\sqrt{\omega_\xi} r) R_{n_r', \ell}(\sqrt{\omega_\xi} r) = \delta_{n_r, n_r'} . \quad (39)$$

By expanding the perturbation by

$$\xi(t, \mathbf{x}) = \sum_{n_r, \ell, m_z} q_{n_r, \ell, m_z}(t) R_{n_r, \ell}(r) Y_\ell^{m_z}(\Omega) , \quad (40)$$

the $q_{n_r, \ell, m_z}(t)$ satisfies,

$$[\partial_t^2 + 2\omega_\xi(2n_r + \ell) + \Lambda + F(t)] q_{n_r, \ell, m_z}(t) = 0 . \quad (41)$$

Since we are interested in the effects of the spherical perturbation, we hereafter take $\ell = 0$ and denote $q_{n_r}(t) = q_{n_r, 0, 0}(t)$.

In Fig. 2, we show the instability mode, $n_r = 3$, for $\kappa = -0.3$ and $\zeta = 0.4$. The figure shows that the perturbation grows for $\mathcal{O}(100)/m$. We also show the corresponding wave function $R_{n_r=3, 0}(r)$. Once the perturbation grows around the I-ball/oscillon, it is expected to be dissociated and breaks up into smaller configurations.

In Fig. 3, we also show the Floquet exponent μ

$$\xi(t + T, \mathbf{x}) = e^{\mu T} \xi(t, \mathbf{x}) , \quad (42)$$

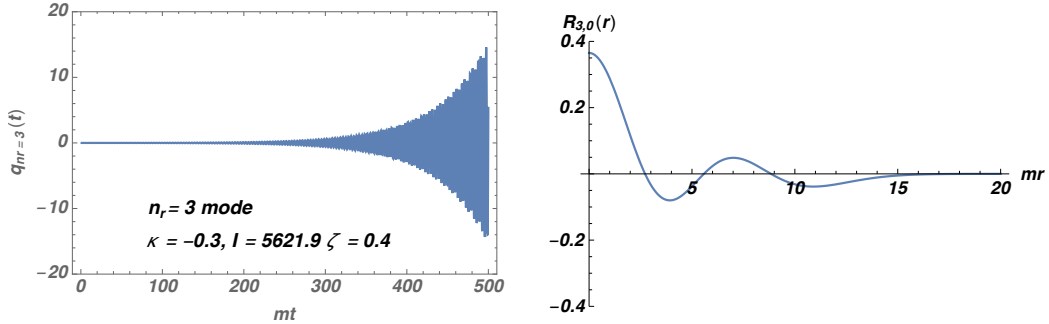


FIG. 2. (Left) The growing mode around the I-ball with $\kappa = -0.3$ and $\zeta = 0.4$. (Right) The corresponding wave function $R_{n_r=3,0}(r)$.

where $T = 2\pi/\omega$ is a period of one oscillation. The figure shows that there are some resonance bands. This means that the exact I-ball/oscillon is not always a stable solution. Thus, in the presence of tiny fluctuations around the exact I-ball/oscillon, the instability modes exhibit the exponential growths in the time scale of $\mathcal{O}(\mu^{-1})$. Once the exponential growth happens, the exact I-ball/oscillon cannot keep its configuration anymore and is expected to be broken up. We will confirm these behaviors by the classical lattice simulation in the next section.

IV. NUMERICAL SIMULATION

A. Setup

In this subsection we briefly explain the setup of the simulation. The procedure of the simulation is similar to that of Ref. [25]. Because the lowest energy configuration of the scalar field ϕ is spherically symmetric in three-dimensional space, the equation of motion of ϕ is represented by

$$\frac{d^2\phi}{dt^2} = \frac{d^2\phi}{dr^2} + \frac{2}{r} \frac{d\phi}{dr} - \frac{\partial V}{\partial\phi}, \quad (43)$$

where

$$V(\phi) = m^2 \left[1 + \kappa \log \left(\epsilon + \frac{\phi^2}{m^2} \right) \right] \phi^2. \quad (44)$$

Here, we introduced a small parameter ϵ to avoid the numerical instability caused by the singularity of the effective mass at $\phi = 0$. We have confirmed that the simulation results are independent of this small regularization term ϵ .

For the boundary condition, we use the two following conditions.

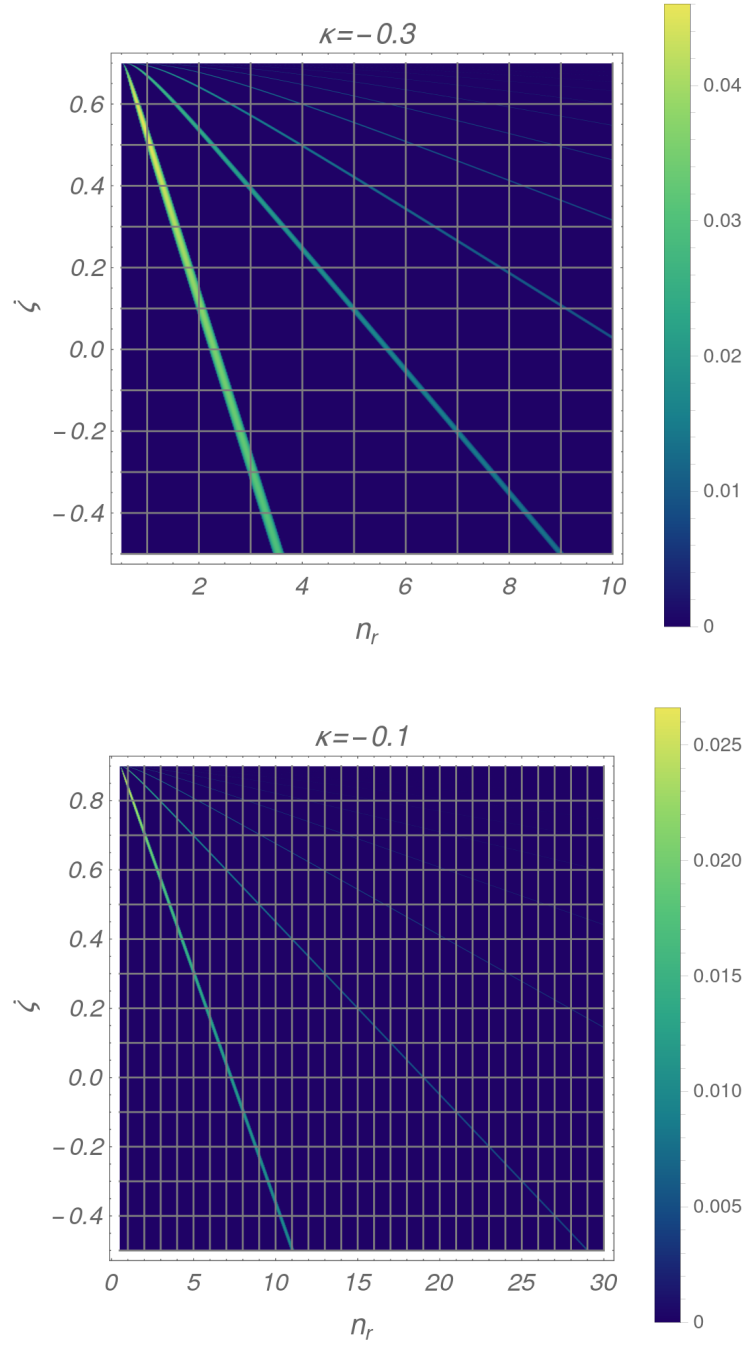


FIG. 3. (upper) Plot of the Floquet exponent μ for the variables n_r and ζ for $\kappa = -0.3$. (lower) Same plot for $\kappa = -0.1$. The instability bands for the spherical modes are at integer values of n_r . The instability bands for the non-spherical modes can be read off by renaming the horizontal axis from n_r to $n_r + \ell/2$.

ζ_{ini}	varying
κ	-0.3
ϵ	10^{-10}
Box size L	64
Grid size N	1024
Initial time	0
Final time	1.0×10^6
Time step	2.0×10^{-3}

TABLE I. Simulation parameters. ζ_{ini} is changed in every simulation to set the appropriate initial profile of the exact I-ball/oscillon.

- At the origin $r = 0$, to avoid the divergence of the second term of the right-hand side of Eq. (43), we impose

$$\left. \frac{1}{r} \frac{d\phi}{dr} \right|_{r=0} = 0. \quad (45)$$

- At the other boundary $r = L$ ($\gg R$), we impose the absorbing boundary condition (see Appendix A for details). Under this condition, the radiation of the real scalar field emitted from the I-ball/oscillon is absorbed at the boundary so that we correctly calculate the time evolution of I-ball/oscillon.

As the initial condition of ϕ , we use the theoretical I-ball/oscillon configuration Eqs. (13)-(15) for a given ζ_{ini} with 1% random fluctuations. We also set

$$\dot{\phi}(t = 0, r) = 0, \quad (46)$$

as an initial condition of $\dot{\phi}$. We have confirmed that the exact I-ball/oscillon is completely stable in the absence of the random fluctuations.

The other simulation parameters are shown in Table I. Here, the units of the field, time, space, etc. are taken to be m^{-1} , that is,

$$\phi \rightarrow m\phi, \quad t \rightarrow \frac{t}{m}, \quad x \rightarrow \frac{x}{m}, \quad \dots \text{ etc.} \quad (47)$$

We utilize the same lattice simulation code in [25], in which the time evolution is calculated by the fourth-order symplectic integration scheme and the spatial derivatives are calculated by the fourth-order central difference scheme.

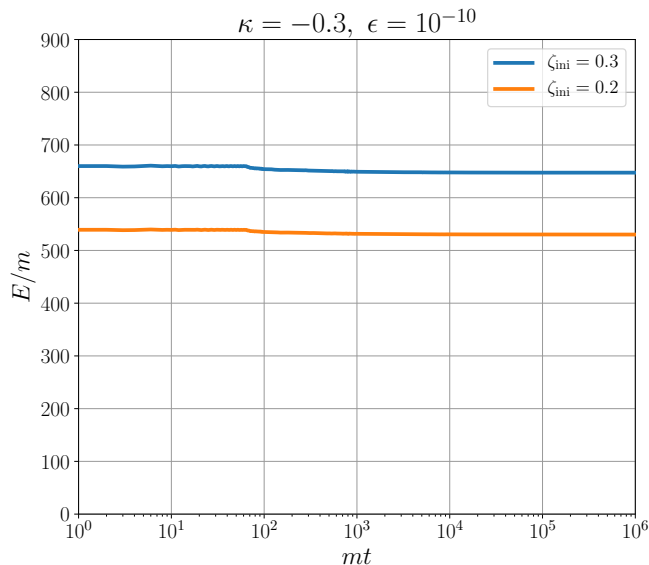


FIG. 4. The result of our simulations for the stable exact I-ball/oscillon. The blue and the orange lines show the exact I-ball/oscillon energy (defined by Eq. (48)) for $\zeta_{\text{ini}} = 0.3$ and $\zeta_{\text{ini}} = 0.2$, respectively. The energy suddenly changes at $mt \simeq 60$ because the radiated fluctuations have reached the boundary and start to be absorbed at that time. We find that the exact I-ball/oscillon energy is conserved in $mt \lesssim 10^6$ when the exact I-ball/oscillon does not have instability modes around it.

B. Result

We numerically calculate the time evolution of the exact I-ball/oscillon ϕ and its energy E from

$$E(t) = \int_0^L dr 4\pi r^2 \left[\frac{1}{2} \dot{\phi}^2 + \frac{1}{2} (\nabla \phi)^2 + V \right], \quad (48)$$

to see how it behaves in the presence of the instability modes derived in Sec. III.

Stability

First, we show the result of the stable exact I-ball/oscillon which has no strong instability resonance bands. The result is given in Fig. 4, which shows that the exact I-ball/oscillation does not break up even in the presence of the tiny fluctuation. This result is consistent with the fact the exact I-ball/oscillon for $\zeta_{\text{ini}} = 0.3, 0.2$ does not have the instability modes.

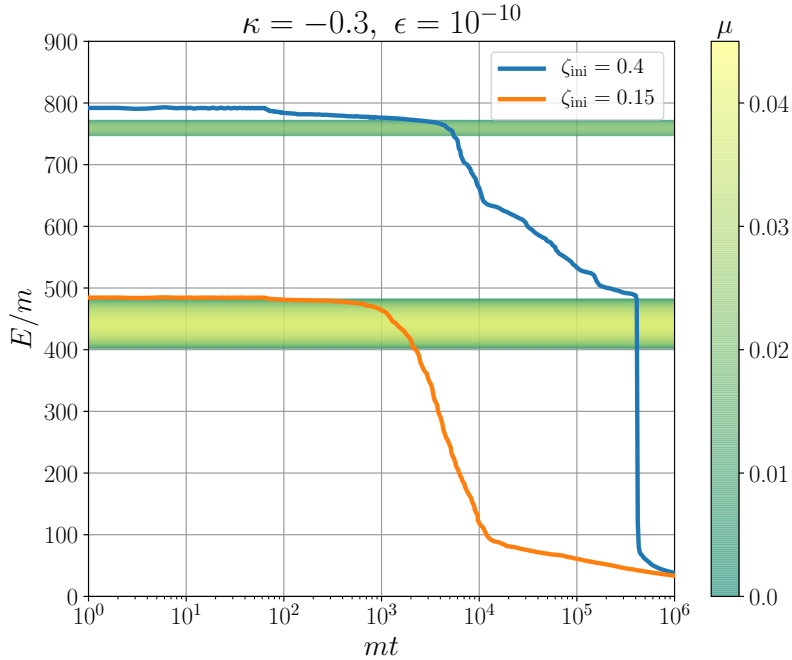


FIG. 5. The result of our simulations for the unstable exact I-ball/oscillon, which hit the instability bands. The blue and the orange lines show the exact I-ball/oscillon energy (defined by Eq. (48)) for $\zeta_{\text{ini}} = 0.4$ and $\zeta_{\text{ini}} = 0.15$ respectively. We also plot the typical instability bands as the Floquet exponent μ exhibited in Fig. 3 by green thick lines. The upper dark green line and the lower bright green line correspond to the instability bands at $\zeta \simeq 0.4$, $n_r = 3$ and $\zeta \simeq 0.1$, $n_r = 2$ in Fig. 3. The sudden change of the energy at $mt \simeq 60$ is for the same reason as the case of Fig. 4. We find that the exact I-ball/oscillon energy strikingly decreases around the instability bands.

Fragileness

Next, we show the result of the unstable exact I-ball/oscillon. The results of the simulations are shown in Fig. 5.⁵ Comparing the result with our analytical calculation (see Fig. 3), we find that the energy of exact I-ball/oscillon strikingly decreases at around instability bands showed as green color bands in Fig. 5. This can be interpreted that the initial fluctuations appended to the exact I-ball/oscillon grow exponentially and deform the exact I-ball/oscillon profile⁶.

Our results also suggest that the exact I-ball/oscillon ends up with another exact I-

⁵ We have confirmed that the exact I-ball/oscillon for the given ζ_{ini} without initial fluctuations is stable within simulation time.

⁶ Instability bands should be wide and strong enough for the oscillon decay.

ball/oscillon profile with a smaller I after the decay process. In fact, both the cases in Fig. 5 converge to the smaller but finite energy at $mt \gtrsim 10^6$. The case with $\zeta_{\text{ini}} = 0.4$ is particularly suggestive. In this case, the I-ball/oscillon first decays when the instability modes in the narrower band around $\zeta = 0.4$ and $n_r = 3$ grows, and ends up with the I-ball/oscillon with $\zeta \simeq 0.15$. However, there is a broader instability band for $\zeta \simeq 0.15$ and $n_r = 2$, with which the exact I-ball/oscillon further decays very quickly. As a result, the exact I-ball/oscillon profile for $\zeta_{\text{ini}} = 0.4$ converges to the smaller I-ball/oscillon solution.

In our analysis, we only consider the radial modes of the fluctuation. The exact I-ball/oscillon can have more instability bands in the three dimensional case (see Eqs. (31) and (41)).

V. CONCLUSIONS

In this paper, we examine the stability of the exact I-ball/oscillon. The exact I-ball/oscillon has been considered to be stable since it has the exactly conserved adiabatic invariant. Its stability is also expected because the perturbations around the exact I-ball/oscillon obey the field equation without the source terms.

However, we have found that the exact I-ball/oscillon is not always a stable solution and the perturbation around it has growth modes depending on the size of the adiabatic invariant. Thus, in the presence of the fluctuations with the corresponding instability modes, the exact I-ball/oscillon cannot keep its configuration anymore and breaks up eventually.

The mechanism of the exact I-ball/oscillon decay in this paper is completely different from the previous study [25], in which I-ball/oscillon decays by emitting relativistic radiations of the scalar field. Our results in this paper suggest that it is necessary to consider both decay processes, the decay by radiation and the decay by the instability modes, when we estimate the lifetime of generic I-ball/oscillon.

ACKNOWLEDGMENTS

This work was supported by JSPS KAKENHI Grant Nos. 17H01131 (M.K.) and 17K05434 (M.K.), MEXT KAKENHI Grant Nos. 15H05889 (M.K., M.I.), No. 16H03991(M.I.), No. 17H02878(M.I.), and No. 18H05542 (M.I.), World Premier International Research Cen-

ter Initiative (WPI Initiative), MEXT, Japan, and JSPS Research Fellowships for Young Scientists Grant No. 19J12936 (E.S.).

Appendix A: Absorbing Boundary Condition

In this appendix, we briefly explain the Absorbing Boundary Condition (ABC) based on the references [20, 34]. We only consider the single real scalar field ϕ for simplicity.

The equation of motion of ϕ is written as

$$\ddot{\phi} - \Delta\phi + \frac{\partial V}{\partial\phi} = 0 \quad (\text{A1})$$

where V is an arbitrary potential of ϕ . Assuming that the field ϕ can be expanded around the minimum $\phi = v$ as

$$\phi = v + \varphi, \quad (\varphi \ll v) \quad (\text{A2})$$

where

$$\left. \frac{\partial V}{\partial\phi} \right|_{\phi=v} = 0, \quad (\text{A3})$$

the equation of motion of ϕ is rewritten as

$$\ddot{\varphi} - \Delta\varphi + m_{\text{eff}}^2\varphi \simeq 0. \quad (\text{A4})$$

where

$$\left. \frac{\partial^2 V}{\partial\phi^2} \right|_{\phi=v} \equiv m_{\text{eff}}^2. \quad (\text{A5})$$

We ignore the higher terms of φ because we consider φ is much smaller than v ⁷.

Assuming the spherical symmetry in three dimensions $\varphi = \varphi(r)$, the equations of motion becomes

$$\ddot{\varphi} - \frac{\partial^2\varphi}{\partial r^2} - \frac{2}{r}\frac{\partial\varphi}{\partial r} + m_{\text{eff}}^2\varphi \simeq 0. \quad (\text{A9})$$

Performing Fourier-transformation of φ as t ,

$$\varphi(t, r) = \int d\omega \varphi(\omega, r) e^{-i\omega t}. \quad (\text{A10})$$

⁷ The potential of ϕ is expanded as

$$V(\phi) = V(v + \varphi), \quad (\text{A6})$$

$$= V(v) + \left. \frac{\partial V}{\partial\phi} \right|_{\phi=v} \varphi + \frac{1}{2} \left. \frac{\partial^2 V}{\partial\phi^2} \right|_{\phi=v} \varphi^2 + \mathcal{O}(\varphi^3), \quad (\text{A7})$$

$$= V(v) + \frac{1}{2} \left. \frac{\partial^2 V}{\partial\phi^2} \right|_{\phi=v} \varphi^2 + \mathcal{O}(\varphi^3). \quad (\text{A8})$$

the equations of motion becomes

$$\left[\frac{\partial^2}{\partial r^2} + \frac{2}{r} \frac{\partial}{\partial r} + (\omega^2 - m_{\text{eff}}^2) \right] \varphi = 0, \quad (\text{A11})$$

$$\Leftrightarrow \left[\frac{\partial}{\partial r} - \left(i\sqrt{\omega^2 - m_{\text{eff}}^2} - \frac{1}{r} \right) \right] \left[\frac{\partial}{\partial r} + \left(i\sqrt{\omega^2 - m_{\text{eff}}^2} - \frac{1}{r} \right) \right] \varphi = 0. \quad (\text{A12})$$

The special solution of this equation at $m_{\text{eff}} r \gg 1$ is Bessel function and

$$\varphi(t, r) = \frac{1}{r} \exp \left[i \left(\pm \sqrt{\omega^2 - m_{\text{eff}}^2} r + \omega t \right) \right]. \quad (\text{A13})$$

The reflected wave must be disappeared at the boundary $r = r_b$ ($m_{\text{eff}} r \gg r_b$),

$$\left[\frac{\partial}{\partial r} - \left(i\sqrt{\omega^2 - m_{\text{eff}}^2} - \frac{1}{r} \right) \right] \Big|_{r=r_b} \varphi = 0. \quad (\text{A14})$$

Expanding the square root,

$$\left[\frac{\partial}{\partial r} - i\omega \left(1 - \frac{1}{2} \frac{m_{\text{eff}}^2}{\omega^2} + \mathcal{O} \left(\left(\frac{\omega}{m_{\text{eff}}} \right)^4 \right) \right) + \frac{1}{r} \right] \varphi = 0, \quad (\text{A15})$$

$$\Leftrightarrow \left[i\omega \frac{\partial}{\partial r} + \left(\omega^2 - \frac{1}{2} m_{\text{eff}}^2 \right) + \frac{i\omega}{r} \right] \varphi \simeq 0. \quad (\text{A16})$$

Substituting $i\omega \rightarrow -\frac{\partial}{\partial t}$

$$\left[\frac{\partial}{\partial r} \frac{\partial}{\partial t} + \frac{\partial^2}{\partial t^2} + \frac{1}{2} m_{\text{eff}}^2 + \frac{1}{r} \frac{\partial}{\partial t} \right] \varphi = 0, \quad (\text{A17})$$

Therefore, $\pi = \dot{\varphi}$ obeys at the boundary $r = r_b$

$$\dot{\pi}(t, r_b) = - \frac{\partial \pi(t, r)}{\partial r} \Big|_{r=r_b} - \frac{1}{2} m_{\text{eff}}^2 \varphi(t, r_b) - \frac{1}{r_b} \pi(t, r_b). \quad (\text{A18})$$

-
- [1] I. L. Bogolyubsky and V. G. Makhankov, *Pisma Zh. Eksp. Teor. Fiz.* **24**, 15 (1976).
[2] M. Gleiser, *Phys. Rev.* **D49**, 2978 (1994), arXiv:hep-ph/9308279 [hep-ph].
[3] E. J. Copeland, M. Gleiser, and H. R. Muller, *Phys. Rev.* **D52**, 1920 (1995), arXiv:hep-ph/9503217 [hep-ph].
[4] J. McDonald, *Phys. Rev.* **D66**, 043525 (2002), arXiv:hep-ph/0105235 [hep-ph].
[5] M. A. Amin and D. Shirokoff, *Phys. Rev.* **D81**, 085045 (2010), arXiv:1002.3380 [astro-ph.CO].
[6] M. A. Amin, R. Easther, H. Finkel, R. Flauger, and M. P. Hertzberg, *Phys. Rev. Lett.* **108**, 241302 (2012), arXiv:1106.3335 [astro-ph.CO].

- [7] M. A. Amin, Phys. Rev. **D87**, 123505 (2013), arXiv:1303.1102 [astro-ph.CO].
- [8] N. Takeda and Y. Watanabe, Phys. Rev. **D90**, 023519 (2014), arXiv:1405.3830 [astro-ph.CO].
- [9] K. D. Lozanov and M. A. Amin, Phys. Rev. Lett. **119**, 061301 (2017), arXiv:1608.01213 [astro-ph.CO].
- [10] F. Hasegawa and J.-P. Hong, Phys. Rev. **D97**, 083514 (2018), arXiv:1710.07487 [astro-ph.CO].
- [11] S. Antusch, F. Cefala, S. Krippendorff, F. Muia, S. Orani, and F. Quevedo, JHEP **01**, 083 (2018), arXiv:1708.08922 [hep-th].
- [12] J.-P. Hong, M. Kawasaki, and M. Yamazaki, Phys. Rev. **D98**, 043531 (2018), arXiv:1711.10496 [astro-ph.CO].
- [13] M. Kawasaki, F. Takahashi, and N. Takeda, Phys. Rev. **D92**, 105024 (2015), arXiv:1508.01028 [hep-th].
- [14] G. Fodor, P. Forgacs, P. Grandclement, and I. Racz, Phys. Rev. **D74**, 124003 (2006), arXiv:hep-th/0609023 [hep-th].
- [15] G. Fodor, P. Forgacs, Z. Horvath, and M. Mezei, Phys. Rev. **D79**, 065002 (2009), arXiv:0812.1919 [hep-th].
- [16] M. Gleiser and D. Sicilia, Phys. Rev. Lett. **101**, 011602 (2008), arXiv:0804.0791 [hep-th].
- [17] G. Fodor, P. Forgacs, Z. Horvath, and M. Mezei, Phys. Lett. **B674**, 319 (2009), arXiv:0903.0953 [hep-th].
- [18] M. Gleiser and D. Sicilia, Phys. Rev. **D80**, 125037 (2009), arXiv:0910.5922 [hep-th].
- [19] M. P. Hertzberg, Phys. Rev. **D82**, 045022 (2010), arXiv:1003.3459 [hep-th].
- [20] P. Salmi and M. Hindmarsh, Phys. Rev. **D85**, 085033 (2012), arXiv:1201.1934 [hep-th].
- [21] P. M. Saffin, P. Tognarelli, and A. Tranberg, JHEP **08**, 125 (2014), arXiv:1401.6168 [hep-ph].
- [22] M. Kawasaki and M. Yamada, JCAP **1402**, 001 (2014), arXiv:1311.0985 [hep-ph].
- [23] K. Mukaida, M. Takimoto, and M. Yamada, JHEP **03**, 122 (2017), arXiv:1612.07750 [hep-ph].
- [24] J. Eby, K. Mukaida, M. Takimoto, L. C. R. Wijewardhana, and M. Yamada, Phys. Rev. **D99**, 123503 (2019), arXiv:1807.09795 [hep-ph].
- [25] M. Ibe, M. Kawasaki, W. Nakano, and E. Sonomoto, JHEP **04**, 030 (2019), arXiv:1901.06130 [hep-ph].
- [26] J. Ollé, O. Pujolàs, and F. Rompineve, (2019), arXiv:1906.06352 [hep-ph].
- [27] S. Antusch, F. Cefalà, and F. Torrentí, (2019), arXiv:1907.00611 [hep-ph].
- [28] S.-Y. Zhou, E. J. Copeland, R. Easther, H. Finkel, Z.-G. Mou, and P. M. Saffin, JHEP **10**,

- 026 (2013), arXiv:1304.6094 [astro-ph.CO].
- [29] S. Antusch, F. Cefala, and S. Orani, Phys. Rev. Lett. **118**, 011303 (2017), [Erratum: Phys. Rev. Lett.120,no.21,219901(2018)], arXiv:1607.01314 [astro-ph.CO].
- [30] K. D. Lozanov and M. A. Amin, Phys. Rev. **D99**, 123504 (2019), arXiv:1902.06736 [astro-ph.CO].
- [31] J. Eby, M. Leembruggen, L. Street, P. Suranyi, and L. C. R. Wijewardhana, (2019), arXiv:1905.00981 [hep-ph].
- [32] S. Kasuya, M. Kawasaki, and F. Takahashi, Phys. Lett. **B559**, 99 (2003), arXiv:hep-ph/0209358 [hep-ph].
- [33] K. Mukaida and M. Takimoto, JCAP **1408**, 051 (2014), arXiv:1405.3233 [hep-ph].
- [34] B. Engquist and A. Majda, Mathematics of Computation **31**, 629 (1977).